DRAFT-IMECE2010-30412

Optothermal Analyte Manipulation With Temperature Gradient Focusing

M. Akbari
Mechatronic System Engineering School of
Engineering Science, Simon Fraser University,
Surrey, BC, V3T 0A3, Canada.

M. Bahrami
Mechatronic System Engineering School of
Engineering Science, Simon Fraser University,
Surrey, BC, V3T 0A3, Canada.

D. Sinton
Department of Mechanical Engineering,
University of Victoria,Victoria, BC, V8W 2Y2,
Canada.

ABSTRACT

An optothermal analyte preconcentration method is introduced in this work based on temperature gradient focusing. The present approach offers a flexible, noncontact technique for focusing and transporting of analytes. Here, we use a commercial video projector and an optical system to generate heat and control the heat source position, size and power. This heater is used to focus a sample model analyte, fluorescent dye, at an arbitrary location along the microchannel. Optothermal manipulation of the focused band was demonstrated by projecting a series of images with a moving light band.

1. INTRODUCTION

Microfluidic systems can be designed to create rapid and efficient portable point-of-care (POC) medical diagnosis systems to obtain and process measurements from small volumes of complex fluids [1-3]. Detecting dilute analytes in microfluidic formats [1-3] generally requires preconcentration prior to separation and/or detection stages [4]. Examples of preconcentration methods include field amplified stacking (FAS) [5-8], isotachophoresis (ITP) [9, 10], sweeping [11-13], electric field gradient focusing (EFGF) [14-16], and temperature gradient focusing (TGF) [4, 17-20].

In TGF, the focusing is achieved by balancing the bulk flow in a channel against the electrophoretic migrative flux of an analyte along a controlled temperature profile. In previous works, the required temperature profile was generated by heating/cooling blocks [4, 17, and 19], peltier elements [18 and 20], and joule heating in a variable cross-section microchannel [4,19]. Here, we use an optothermal heating method [21] to concentrate and manipulate analytes. Major advantages associated with the proposed heating method include control of the size, location and shape of the temperature profile, and also the ability to generate localized heating without need for integrated heating/cooling components, provides the ability to generate a tightly concentrated band in a very short microchannel and transport it to the point of analysis, on demand. Since the proposed method is contactless, predefined geometries, complex fabrication and controlling systems are avoided. Moreover, using lower applied voltages for concentration is possible which prevents unstable focused bands due to the "thermal run away" effect which is common in the systems using the joule heating effect [19].

2. EXPERIMENTAL RESULTS

In our experiments, an inverted epi-fluorescent microscope (Jenco, Oregon) with 5X, 0.12 N.A. long distance objective, rhodamine B (excitation: band pass 546 nm, emission: band pass 600 nm) and green (excitation: band pass 540 nm, emission: band pass 580 nm) filter sets, a broadband mercury illumination source, and a digital CCD camera were used. Image acquisition and storage was controlled by Zarbco video toolbox (Ver. 1.65) software. Ultra-small pressure driven flow, (flow rates on the order of $\sim 1 \mu L/hr$), were produced using hydrostatic pressure (i.e. difference between two columns of water). A commercial video projector (Sony, 3-LDC BrightEra, 190 W Mercury lamp, 1600/2000 ANSI lumens) equipped with special optics were used for optothermic control of the system. A 50 mm long rectangular borosilicate glass capillary (Vitrocom, NJ) with nominal inner dimensions of $20 \times 200 \ \mu m$ was used as the microchannel. The capillary was mounted on a microscope slide ($25 \ mm \times 75 mm \times 1 mm$) using an acrylic double sided tape (Adhesives Research, Inc., Arclad 8102 transfer adhesive). Pipette tips were cut, inverted (wide side down), and epoxied at the channel ends to interface to the external fluidics. A black electric tape was fixed on the surface of the microchannel, providing a light absorbing material. Images were projected onto the surface of the black tape using the abovementioned optical setup controlled by a laptop.
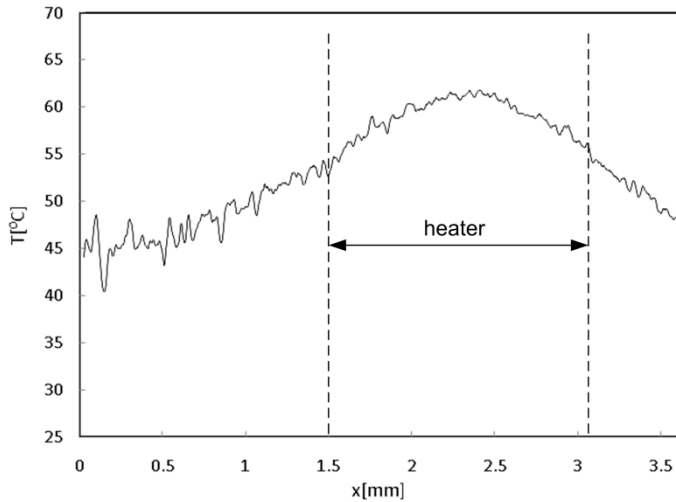
Figure 1. Measured temperature distribution along a microchannel spanning the 3.5-mm field of view of the microchannel. The heat source is approximately $1.5\ mm$ wide. At each axial location, the cross-sectional average of the temperature field is shown.

We performed *in situ* temperature field imaging based upon the temperature-dependent quantum efficiency of rhodamine B, using the method introduced by Ross and co-workers [22] and described in our previous work [21]. Briefly, 0.1 mM rhodamine B in 900 mM Tris-borate buffer solution was prepared and introduced into the microchannel. A background and an isothermal "cold field" intensity image of the system were taken prior to each experiment. Following the acquisition of the cold field image, the prescribed pressure driven flow was set and a rectangular strip of light was projected on the surface of the black tape to provide a localized heating. The heat source width was estimated to be $1.5\ mm$. Images were taken every 2 seconds with the resolution of 1280×1024 pixels, spanning a length of $3.5\ mm$ of the channel. To extract the in-channel temperature profiles, background image was first subtracted from each raw image and the cold field. The corrected raw images were then normalized with the corrected cold field images. The intensity values of the treated images were then converted to temperature using the intensity vs. temperature calibration, as described by [21]. Figure 1 shows the Gaussian shape steady state temperature profile for no-flow condition along the microchannel produced by a heater size of approximately $1.5\ mm$, after taking cross-sectional averaging at each axial location. Our temperature measurements [21] show that by increasing the flow rate, the peak in temperature slightly decreases and shifts to the downstream of the flow.

The thermal response of the microfluidic system plotted in Figure 2 indicates that our heating system reaches the steady-state condition with the rate of approximately $1\ ℃/s$. Maximum temperature rise in Figure 2, $T - T_{amb}$, was obtained by finding the maximum value of the cross-sectional averaged temperature profile at each time.
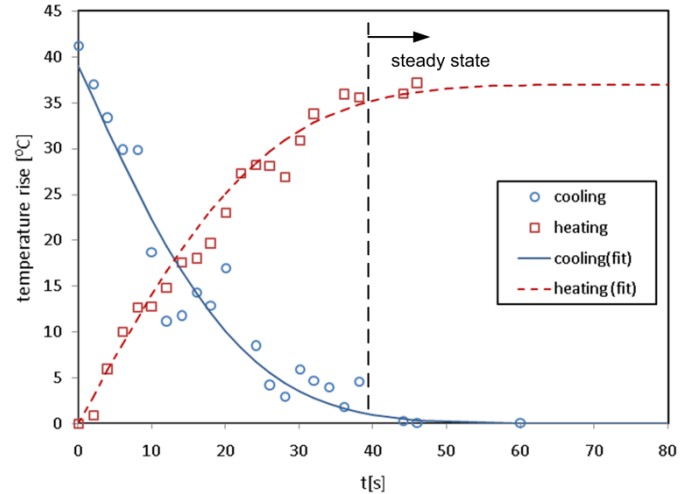
Figure 2. Variation of maximum temperature rise, $T - T_{amb}$, vs. time for no-flow condition and stationary heater. The heater width is approximately 1.5 mm for this plot. Each data point is obtained by finding the maximum temperature along the microchannel. Temperature at each axial location is obtained by taking the cross-sectional average.

Focusing experiments were performed using 0.1mM Fluorescein in 900 mM Tris-borate buffer at pH 8. Before each experiment, the channel and reservoirs were flushed with distilled water and buffer for at least $15\ min$. Both reservoirs were emptied and 0.1mM Fluorescein solution was introduced in one reservoir and the channel was allowed to fill with the hydrostatic pressure. Then the other reservoir was filled with Fluorescein and the pressure head was applied. The heat source was projected on the surface of the black tape, electric field was switched on after the steady state temperature was obtained, and image acquisition was performed every 20 seconds. After electric potential was applied to the channel the pressure head was tuned until the focused band was observed.

Parts a to f in Figure 3 show the focusing of Fluorescein after applying $200\ V/cm$ electric field. Images were taken every 20 seconds and exported to an in-house Matlab code for post processing. Initially, the microchannel was filled with a diluted sample solution (0.1 mM in Tris-Borate, PH 8) uniformly distributed within the channel. It can be seen that after 6 minutes, concentration of the Fluorescein is significantly increased under the heat source. Figure 3-g shows the variation of axial concentration profile with time. At each axial location cross-sectional averaging was performed. It should be noted that the optothermal heating system used in this work is able to control the location of the heat source. As a result, the location of focused band along the microchannel can be determined on-demand without any need for pre-defined geometry or complex controlling system. Moreover, since the size of the heat source can be shrunk down, shorter preconcentration channels are required, thus significantly smaller microchannel footprint is needed.
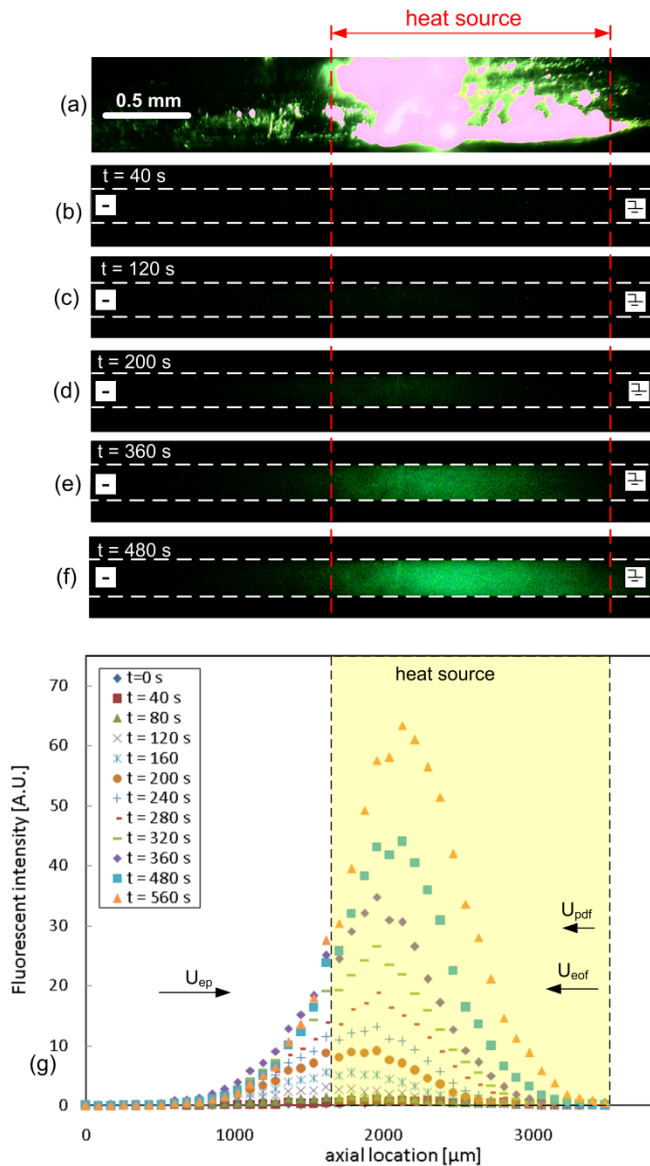
Figure 3. Images of sample analyte focusing with an applied electric field of 200 V/cm. (a) heat source location under the microscope, (b) channel after 40 sec, (c) channel after 120 sec , (d) channel after 200 sec, (e) channel after 360 sec, (f) channel after 480 sec, and (g) transient variation of Fluorescent intensity profile along the microchannel. Pressure driven velocity is in the order of 0.15 mm/s in favour of the electroosmotic flow from right to left.

The measured peak concentration versus time for two runs is plotted in Figure 4. The peak concentration for each of the two runs follow a roughly linear increase as predicted by Ross et al. [4]. Normalized concentration in this plot is defined as $I(t)/I_0$ where I_0 is the initial intensity (corresponds to 0.1 mM concentration) and $I(t)$ is the measured intensity at anytime. As can be seen, more than 50-fold enrichment in 12 minutes is obtained for Fluorescein as the analyte model.
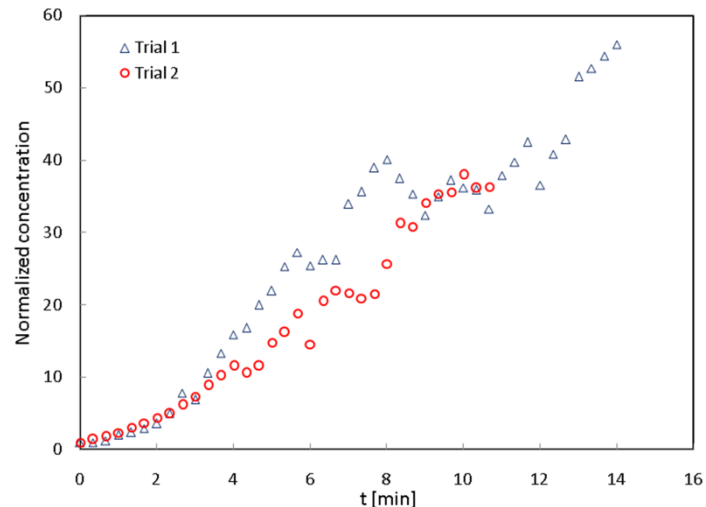
Figure 4. Peak sample concentration vs. time for two different focusing runs. Normalized concentration at each time is defined as the ratio of fluorescent intensity at that time over the initial fluorescent intensity. More than 50-folds enrichment in concentration is obtained in almost 12 mistunes.

On-demand transport of the focused band along the microchannel was performed by moving the heat source. Figure 5 shows the image sequence of the fluorescein band transport in two directions. The applied electric field for both directions was 160 V/cm with the same electrode polarity. The direction and magnitude of the pressure driven flow was also remained unchanged. To ensure the stability of the focused band at the initial location (i.e. point A), image sequences were taken every 2 seconds for 3 minutes and the location of the peak concentration was monitored. Then the heat source was transferred 500 μm every 3 minutes to generate a quasi-steady moving heat source. As can be seen, the focused band is following the heat source in both directions indicating the successful transport of the focused band from point A to B, and back. It should be noted that the advantage of present method compared to conventional concentration methods such as such as sample stacking is that both stationary and moving focused bands can be generated by this method, transporting of the focused sample in both directions is possible with only one background buffer, and the instabilities that can occur at the interface between high/low concentrations is avoided.

3. CONCLUSION

We presented an optothermal analyte manipulating method based on temperature gradient focusing that enables dynamic control of the focused band location and its on-demand transportation to the point of analysis. Moreover, using this optothermal technique shorter preconcentration channels are required compared to other heating techniques used in TGF in previous works. The proposed method was demonstrated using a sample model analyte, fluorescent dye. More than 50-fold enrichment in concentration of fluorescein was achieved in under 14 minutes. Since the location of the heated area is

controllable, the focused band can be generated at any point along the microchannel without integrated heaters/coolers of predefined geometry or a complex control system. We also demonstrated the on-demand manipulation of the focused band by projecting a translating image and thus moving the optothermal heat source. This ability of the system can be used for sequential concentration and separation of different analytes and transporting the focused bands to the point of analysis.
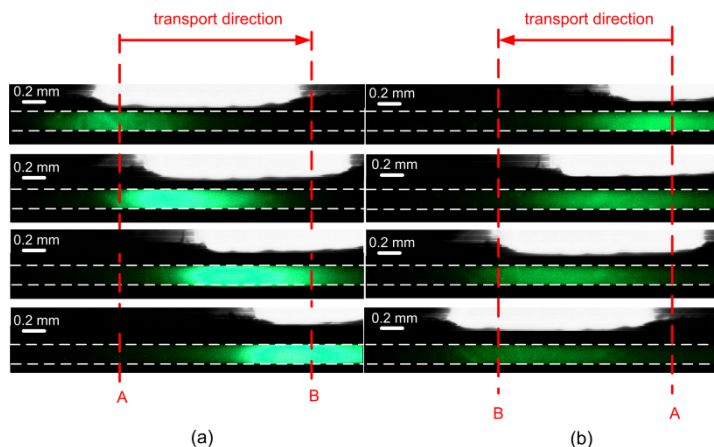
Figure 5. Image sequences showing the on-demand transport of Fluorescein focused band from point A to B by moving the heat source. (a) from left to right and (b) from right to left. Applied electric field is 160 V/cm, the left hand side electrode polarity is negative, and the right hand side electrode is grounded for both directions. Stable focused band is first generated at point A (the stability is examined by processing a sequence of images taken every 2 seconds for 3 minutes) and then transported to point B following the heat source. The direction and magnitude of the pressure driven flow was remained unchanged during the experiments.

ACKNOWLEDGMENTS

REFERENCES

[1] Yager, P, Edwards, T., Fu, E., Helton, K., Nelson, K., Tam, M.R., and Weigl, B.H., Microfluidic diagnostic technologies for global public health, Nature 442 (2006) 412–418.

[2] Dupuy, A., Lehmann, S., and Cristol, J., Protein biochip systems for the clinical laboratory, Clin. Chem. Lab. Med. 43 (2005) 1219-1302.

[3] Toner, M. and Irimia, D., Blood-on-a-chip, Annu. Rev. Biomed. Eng. 7 (2005) 77-103.

[4] Ross, D. and Locascio, L.E., Microfluidic temperature gradient focusing, Anal. Chem. 74 (2002) 2556-2564.

[5] Mikkers, F. E. P., Everaerts, F. M., and Verheggen, P. E. M., High-performance zone electrophoresis, J. Chromatgr. 169 (1979) 11 – 20.

[6] Burgi, D. S. and Chien, R.-L., Optimization in sample stacking for high-performance capillary electrophoresis, Anal. Chem. 63 (1991) 2042 – 2047.

[7] Chien, R.-L., and Burgi, D. S., Sample stacking of an extremely large injection volume in high-performance capillary electrophoresis, Anal. Chem. 64 (1992) 1046 – 1050.

[8] Albert, M., Debusschere, L., Demesmay, C., and Rocca, J. L., Large-volume stacking for quantitative analysis of anions in capillary electrophoresis I. Large-volume stacking with polarity switching , J. Chromatgr.A 757 (1997) 281 – 289.

[9] Boček, P., Deml, M., and Janák, J., Effect of a concentration cascade of the leading electrolyte on the separation capacity in isotachophoresis, J. Chromatogr.156 (1978) 323 – 326.

[10] Everaerts, F. M., Verheggen, P. E. M., and Mikkers, F. E. P., Determination of substances at low concentrations in complex mixtures by isotachophoresis with column coupling, J. Chromatogr. 169 (1979) 21 – 38.

[11] Quirino, J. P. and Terabe, S., Exceeding 5000-fold concentration of dilute analytes in micellar electrokinetic chromatography, Science 282 (1998) 465 – 468.

[12] Quirino, J. P. and Terabe, S., Sweeping of analyte zones in electrokinetic chromatography, Anal. Chem. 71 (1999) 1638 – 1644.

[13] Isoo, K. and Terabe, S., Analysis of metal ions by sweeping via dynamic complexation and cation-selective exhaustive injection in capillary electrophoresis, Anal. Chem. 75 (2003) 6789 – 6798.

[14] Koegler, W. S. and Ivory, C. F., Focusing proteins in an electric field gradient, J. Chromatgr. A 726 (1996) 229 – 236.

[15] Tolley, H. D., Wang, Q., LeFebre, D. A., and Lee, M. L., Equilibrium gradient methods with nonlinear field intensity gradient: a theoretical approach, Anal. Chem. 74 (2002) 4456 – 4463.

[16] Astroga-Wells, J., Vollmer, S., Tryggvason, S., Bergman, T., and Jőrnvall, H., Microfluidic electrocapture for separation of peptides, Anal. Chem. 2005, 77, 7131 – 7136.

[17] Balss, K.M., Vreeland, W.N., Howell, P.B., Henry, A.C., and Ross, D., Micellar affinity gradient focusing: a new method for electrokinetic focusing, J. Am. Chem. Soc. 126 (2004) 1936-1937

[18] Huber, D. and Santiago, J.G., Taylor–Aris dispersion in temperature gradient focusing, Electrophoresis 28 (2007) 2333-2344.

[19] Sommer, G.J., Kim, S.M., Littrel, R.J., and Hasselbrink, E.F., Theoretical and numerical analysis of temperature gradient focusing via joule heating, Lab on a Chip 7(2007) 898-907.

[20] Matsui, T., Franzke, J., Manz, A., and Janasek, D., Temperature gradient focusing in a PDMS/glass hybrid microfluidic chip, Electrophoresis 28 (2007) 4606–4611.

[21] Akbari, M., Bahrami, M., and Sinton , D., Optothermal control of local fluid temperature in microfluidics, Proceeding of ICNMM2010, paper no. FEDSM-ICNMM2010-30412

[22] Ross, D., Johnson T. J., and Locascio, L. E., Temperature measurement in microfluidic systems using a temperature dependent fluorescent dye, Anal. Chem. 73 (2001) 2509–2515.